2018 26th Mediterranean Conference on Control and Automation (MED)
Zadar, Croatia, June 19-22, 2018

Sensitivity based event-triggered TDMA protocol for distributed optimization

Shaban Guma[1] and Naim Bajcinca[2]

Abstract— **We present the design of a sensitivity based event-triggered TDMA protocol in conjunction with a distributed optimization algorithm utilizing dual subgradient method. The event-triggered protocol is based on a sensitivity analysis and it regards the impact of the information exchange into the evolution of the optimization algorithm. The proposed algorithm is evaluated in the context of distributed feedforward control of vehicle dynamics.**

I. INTRODUCTION

In the context of distributed wireless networked control systems, the efficient use of communication and computation resources is of key importance to ensure the system's performance. However, typical time-driven control policies and communication protocols, being independent of the system's state evolution often times may result in unnecessary high utilization of resources [1]. Introducing an event-based communication mechanism in a distributed system results in a purposeful reduction of the communication in accordance with the dynamic evolution of the local subsystem state. Therefore, a motivation for event-triggered protocols in distributed systems lies in the adjustment from periodic time-based to aperiodic event-based communication in order to accommodate the limited wireless network communication resources.

A variety of event-triggered mechanisms have been suggested in the context of a large-scale wireless distributed system. For instance, a widely used event-triggered mechanisms is based on the novelty content of the local state as defined by a predefined threshold [2]. Motivated by the stabilization goal, some other protocols utilize stability margin levels to design event-triggered conditions [3]. In the context of wireless sensor networks, the work in [4] uses the difference between a two successive measurements as a triggering condition for the next measurement transmission. In [5], [6] a model predictive control strategy combined with an event-triggered condition was introduced as part of a resource-aware control policy and communication scheduling for the wireless control networks. In recent years, the control literature has largely grown by many ideas balancing between the communication and control resource loading in both, embedded and wireless network systems. The present paper introduces another approach that fits into such a class of OSI cross-layer algorithms.

[1]Shaban Guma, University of Kaiserslautern, 67663 Kaiserslautern, Germany guma@rhrk.tu-kl.de
[2]Naim Bajcinca, University of Kaiserslautern, 67663 Kaiserslautern, Germany naim.bajcinca@mv.uni-kl.de

A more specific purpose of the event-based communication and control over the wireless channel, as followed by the authors over the past few years, has been overcoming its difficulties with the real-time specifications. Behind this approach there is always a hope that certain loss of system performance is justifiable by an essential reduction of the communication effort. For instance, the authors' previous work [7] proposed an event-triggered optimization algorithm for distributed feedforward control of vehicle dynamics, where the connected nodes communicate only if the internal state error crosses a predefined threshold. Despite the essential decrease in the communication effort, it was shown that the loss of performance has deteriorated only slightly as a consequence thereof, while providing real-time control performance. Here, we extend the work by introducing an event-triggered adaptive Time Division Multiple Access (TDMA) protocol. The protocol is based on the estimation of the potential effect of an information transmission prior to its completion. To this end, we utilize the idea of sensitivity analysis, which we couple to a subgradient distributed optimization algorithm, solving the control optimization problem at hand. Our protocol conducts then a transmission only after it estimates that its impact in the evolution of the algorithm at the application layer is sufficiently large.

Another contribution of interest of our paper, which is independent of the protocol design, relates to an analytical solution for the optimal tire force allocation for a prescribed maneuver. This solution generalizes the authors' result in [8], where the optimal tire forces have been analytically parametrized in terms of the Lagrange dual variables. While in the present paper, we rather consider the minimization of the adhesion tire variable, it turns out that optimal forces result in simple analytical forms. This given, the outcome holds only in the dual problem analysis and is of benefit for real-time implementation.

The paper is organized as follows. Section II provides the preliminary matter regarding the investigated optimization problem, vehicle dynamics, and the subgradient optimization algorithm. In section III, we present the details of the optimal control problem and its distributed setting. In Section IV we present our adaptive TDMA cross-layer protocol. Finally, in Section V, the simulation results are presented and discussed.

II. OPTIMIZATION PROBLEM AND VEHICLE DYNAMICS - REVIEW

A. Optimization problem

We consider a convex optimization problem, with a cost function being represented by finite set of convex functions

978-1-5386-7891-6/18/$31.00 ©2018 IEEE

$f_0^i(x_i)$, involving convex inequality constraints $f_p(x) \le 0$, and affine equality constraints $h_q(x) = 0$:

$$\begin{aligned} \underset{x}{\text{minimize}} \quad & J_0(x) = \sum_i f_0^i(x_i) \\ \text{subject to} \quad & f_p(x) \le 0,\ p = 1, \dots, n_p \\ & h_q(x) = 0,\ q = 1, \dots, n_q. \end{aligned} \tag{1}$$

Here, $x_i \in \Re^{n_i}$ and n_i represent the local state and its state space dimension, respectively, corresponding to a node of the network. Such a problem setting is typically non-decomposable as the constraints couple the state x_i to some x_j (associated with some other node j from the neighborhood of the ith node, $\mathcal{N}_i$). Note that later for decomposition purposes we often use the designation $\hat{x}_j$ assigned to x_j, indicating a received copy of the variable x_j at the ith node.

B. Dual subgradient method

In general, solving an optimization problem in a distributed setting involves the Lagrangian $L(x, \lambda_p, \nu_q)$ of the primal problem (1), which is given by:

$$L(x, \lambda_p, \nu_q) = \sum_i f_0^i(x_i) + \sum_p \lambda_p f_p(x) + \sum_q \nu_q h_q(x), \tag{2}$$

where $\lambda_p \ge 0$ and ν_q are the dual multiplier variables associated with equality and inequality constraints. The dual function, define by $g(\lambda_p, \nu_q) = \inf_x L(x, \lambda_p, \nu_q)$ is then used to formulate the dual optimization problem:

$$\begin{aligned} \text{maximize} \quad & g(\lambda_p, \nu_q) \\ \text{subject to} \quad & \lambda_p \ge 0. \end{aligned} \tag{3}$$

To solve the dual problem we use the subgradient method [9]. Thereby, we need to update the dual variables λ_p and ν_q in an iterative manner as follows:

$$\begin{aligned} \lambda_p[k+1] &= (\lambda_p[k] - \alpha f_p[k])_+, \\ \nu_q[k+1] &= \nu_q[k] - \alpha h_q[k], \end{aligned} \tag{4}$$

where $x_+ := \max(0, x)$ stands for the projection, k is the subgradient iteration counter and α the step size. The subgradients $f_p[k]$, and $h_q[k]$ are defined as:

$$\begin{aligned} f_p[k] &= -f_p(x^*[k]), \\ h_q[k] &= -h_q(x^*[k]), \end{aligned} \tag{5}$$

where the right-hand side argument $x^*[k] = x^*(\lambda_p[k], \nu_q[k])$ amounts to the current optimal value of the primal variables at the time instant k, i.e.:

$$x^* = \arg \inf_x L(x, \lambda_p[k], \nu_q[k]). \tag{6}$$

C. Vehicle dynamics

We recall the vehicle dynamics background from the author's previous work [7], [10], where an optimal control problem of vehicle dynamics is formulated and solved using a primal subgradient method. Specifically, a planar motion of a vehicle with $N = 4$ wheels is considered, where an independent torque τ_i and steering angle θ_i inputs are applied to each wheel. The vehicle body states described by longitudinal speed v_x, lateral speed v_y, and yaw rate ω_v, while the pitch and roll motion are neglected. At the center of gravity (CG), the vehicle dynamics in the xyz reference is defined as follows:

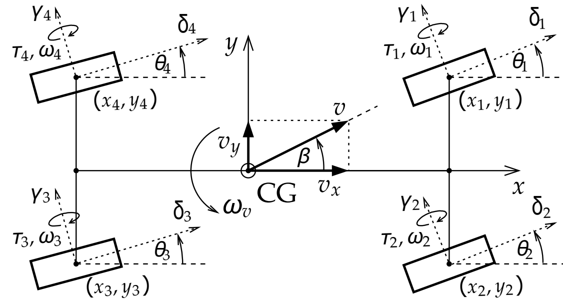

Fig. 1. Inputs and states of the planar vehicle motion.

$$\text{rigid chassis: } M\dot{\xi} = g(\xi) + A_\delta(\theta)F_\delta + A_\gamma(\theta)F_\gamma \tag{7}$$

$$\text{four wheels: } I_w \dot{\omega}_i = r_w F_{i\delta} + \tau_i \tag{8}$$

$$\text{tire model: } F_{i\delta} = f_\delta(\lambda_i, N_i), F_{i\gamma} = f_\gamma(\lambda_i, N_i). \tag{9}$$

The force and moment balance are expressed in the chassis xyz coordinate, with $\xi^T = [v_x, v_y, \omega_v]$, and the vector $g(\xi)$ is caused by the yaw motion $g(\xi) = m_v[\omega_v v_y, -\omega_v v_x, 0]^T$. The force vectors F_δ and F_γ include the lateral $F_{i\delta}$ and longitudinal $F_{i\gamma}$ tire friction forces of the wheel *i*. In (7) the wheel i friction forces' are transformed into the xyz frame by means of the matrices $A_\delta(\theta)$ and $A_\gamma(\theta)$, which are determined by the geometrical parameters (wheelbase and track width) of the vehicle, see [11], [12]. The vector θ includes steering angles θ_i, and $M = \text{diag}[m_v, m_v, I_v]$ is the mass matrix, where, m_v is the vehicle mass, and I_v is the chassis moment of inertia about CG. The rotational motion of the wheel *i* about its own axis γ_i, ω_i stands for its rotational speed. I_w is the wheel moment of inertia, and r_w the effective wheel radius. The functions f_δ and f_γ depend on the specific tire model, and assuming that roll and pitch angle of the vehicle remain identically zero, the normal tire forces N_i in (9) are uniquely determined by the planar forces F_δ and F_γ is computed as follows:

$$N_i = c + P_\delta(\theta)F_\delta + P_\gamma(\theta)F_\gamma, \tag{10}$$

where, the constant vector c and matrices P_δ, P_γ are determined by the vehicle parameters [11]. The dependency of $F_{i\delta}$ and $F_{i\gamma}$ on the normal force N_i is based on friction coefficient $\mu_i^T = [\mu_{i\delta}, \mu_{i\gamma}] \le \mu_{\max}$ which determines the transmission of the lateral and longitudinal tire forces to the vehicle body for a fixed slip λ_i, and $\mu_{\max}$ depends on the road conditions.

The adhesion utilization η_i is defined as the ratio between the magnitude of a tire force and its normal force:

$$\eta_i := \|\mu_i\| = \frac{\|F_i\|}{N_i}, \quad i = 1, \dots, N. \tag{11}$$

where, $0 \le \eta_i \le \mu_{\max}$ represents a feasibility physical condition. This variable reflects the force generation load of a tire.

III. Distributed optimization

A. Dual problem and subgradient algorithm

We consider a system consisting of $N = 4$ independent single actuation units for the manipulation of the vehicle dynamics. Each such unit consists of a local optimization task, whose task is to compute the corresponding optimal tire force allocation (F^*_{ix}, F^*_{iy}), and the adhesion utilization η^*_i. More specifically, the objective of the optimal control problem is achieving the smallest possible utilization of the adhesion potential η_i, while respecting the adhesion limit, thus ensuring an optimal safety reserve in every driving situation, see [12]. Therefore, the optimization problem is defined to penalize the adhesion potentials η_i

$$\begin{aligned}
\underset{\eta_i, F_{xi}, F_{yi}}{\text{minimize}} \quad & J_0 = \sum_{i=1}^{N} \eta_i^2 + \epsilon^2 \left(F_{xi}^2 + F_{yi}^2\right), \\
\text{subject to} \quad & f_1 = \sqrt{F_{xi}^2 + F_{yi}^2} - \eta_i N_i \leq 0, \\
& f_2 = \eta_i - \mu_{\max} \leq 0, \\
& h = A_x F_x + A_y F_y - Y_d = 0.
\end{aligned} \tag{12}$$

Obviously, η_i, and the longitudinal and lateral forces F_{xi} and F_{yi} are considered as decision variables, while $\epsilon \ll 1$ is a regularization term of the optimization problem. A_x and A_y matrices are defined by vehicle geometric parameters, and Y_d is the reference trajectory, $\hat{F}_{xj}$ is the received longitudinal forces vector, $\hat{F}_{yj}$ is the received lateral forces vector, N_i is the normal force, and $\mu_{\max}$ is the maximum friction coefficient parameter. The Lagrangian of the primal problem reads now:

$$\begin{aligned}
L(\eta, F_x, F_y, \lambda, \sigma, \nu) = & \sum_{i=1}^{N} \eta_i^2 + \epsilon^2 \left(F_{xi}^2 + F_{yi}^2\right) \\
& + \sum_{i=1}^{N} \lambda_i\left(\sqrt{F_{xi}^2 + F_{yi}^2} - \eta_i N_i\right) + \sum_{i=1}^{N} \sigma_i(\eta_i - \mu_{\max}) \\
& + \nu^T (A_x F_x + A_y F_y - Y_d),
\end{aligned} \tag{13}$$

with η, $F_x = (F_{x1}, \ldots, F_{x4})^T$, $F_y = (F_{y1}, \ldots, F_{y4})^T$ being primal, and $\lambda_i, \sigma_i, \nu = (\nu_1, \nu_2, \nu_3)$ dual variables. We see that the optimization problem (12) couples the N sub-problems in the equality constraints $h = A_x F_x + A_y F_y - Y_d = 0$.

For breaking the problem (12) into smaller subproblems, [13], we need to introduce local copies ν^i of the global dual variable ν to each sub-problem i. The distributed optimization sub-problem i reads then as follows:

$$\begin{aligned}
\underset{\eta_i, F_{xi}, F_{yi}}{\text{minimize}} \quad & f_0^i = \eta_i^2 + \epsilon^2 \left(F_{xi}^2 + F_{yi}^2\right), \\
\text{subject to} \quad & f_1^i = \sqrt{F_{xi}^2 + F_{yi}^2} - \eta_i N_i \leq 0, \\
& f_2^i = \eta_i - \mu_{\max} \leq 0, \\
& h^i = A_x F_x^i + A_y F_y^i - Y_d = 0.
\end{aligned} \tag{14}$$

Observe that $\hat{F}_x^i$, $\hat{F}_y^i$, $\hat{\eta}_j^i$ refer to the local copies at the node i. The Lagrangian L_i of the sub-problem i is defined as:

$$\begin{aligned}
L_i(\eta_i, F_{xi}, F_{yi}, \lambda_i, \sigma_i, \nu_i) = \eta_i^2 + \epsilon^2 \left(F_{xi}^2 + F_{yi}^2\right) + \\
\lambda_i\left(\sqrt{F_{xi}^2 + F_{yi}^2} - \eta_i N_i\right) + \sigma_i(\eta_i - \mu_{\max}) \\
+ \nu_i^T (A_x \hat{F}_x^i + A_y \hat{F}_y^i - Y_d), \quad j \in \mathcal{N}_i,
\end{aligned} \tag{15}$$

with the corresponding dual function given by:

$$\begin{aligned}
g_i(\lambda_i, \sigma_i, \nu_i) = \inf_{\eta_i, F_{xi}, F_{yi}} \Big(\eta_i^2 + \epsilon^2 \left(F_{xi}^2 + F_{yi}^2\right) + \\
\lambda_i\left(\sqrt{F_{xi}^2 + F_{yi}^2} - \eta_i N_i\right) + \sigma_i \eta_i + \\
\nu_i^T (A_x \hat{F}_{xj} + A_y \hat{F}_{yj})\Big) - \nu_i^T Y_d - \sigma_i \mu_{\max},
\end{aligned} \tag{16}$$

invoking the dual optimization problem:

$$\begin{aligned}
\text{maximize} \quad & g_i(\lambda_i, \sigma_i, \nu_i) \\
\text{subject to} \quad & \lambda_i \geq 0, \\
& \sigma_i \geq 0.
\end{aligned} \tag{17}$$

Using the subgradient method to solve the dual optimization problem (17), we have:

$$\begin{aligned}
\lambda_i[k+1] &= (\lambda_i[k] - \alpha f_1^i[k])_+, \quad i = 1, \ldots, n \\
\sigma_i[k+1] &= (\sigma_i[k] - \alpha f_2^i[k])_+, \quad i = 1, \ldots, n \\
\nu_i[k+1] &= \nu_i[k] - \alpha h^i[k], \qquad i = 1, \ldots, n.
\end{aligned} \tag{18}$$

The subgradients of $f_1[k], f_2[k]$, and $h[k]$ are defined as:

$$\begin{aligned}
f_1^i[k] &:= -f_1^i(\eta^*[k], F_x^*[k], F_y^*[k]), \\
f_2^i[k] &:= -f_2^i(\eta^*[k], F_x^*[k], F_y^*[k]), \\
h^i[k] &:= -h^i(\eta^*[k], F_x^*[k], F_y^*[k]),
\end{aligned} \tag{19}$$

where, as it turns out, the following analytical expressions are valid:

$$\begin{aligned}
\eta_i^*(\lambda_i, \sigma_i) &= \frac{1}{2}\left(\lambda_i N_i - \sigma_i\right), \\
F_{xi}^*(\lambda_i, \nu_i) &= \frac{\kappa_{xi}}{2\epsilon^2}\left(\frac{\lambda_i}{\sqrt{\kappa_{xi}^2 + \kappa_{yi}^2}} - 1\right), \\
F_{yi}^*(\lambda_i, \nu_i) &= \frac{\kappa_{yi}}{2\epsilon^2}\left(\frac{\lambda_i}{\sqrt{\kappa_{xi}^2 + \kappa_{yi}^2}} - 1\right),
\end{aligned} \tag{20}$$

with

$$\kappa_{xi} = \sum_{\ell=1}^{3} \nu_\ell A x_{\ell i}, \qquad \kappa_{yi} = \sum_{\ell=1}^{3} \nu_\ell A y_{\ell i}. \tag{21}$$

In addition to the importance for the real-time implementation of the algorithm at hand due to avoidance of the iterative structures for computation of the primal solutions to (6), notice that the latter analytical expressions share a fundamental character in terms of vehicle dynamics control as they provide an analytical parametrization of the optimal solution for the tire force allocation.

B. Distributed setting and event-triggered communication

Due to the coupling of the N distributed sub-problems via the equality constraint $h(F_x, F_y) = 0$, a distribution of the optimization problems can be accomplished only by introducing the local copies of the variable ν^i of the global variable $\nu_i = [\nu_1, \nu_2, \nu_3]^T$ at every node $i = 1, \ldots, N$, and, additionally, an average consensus step involving an exchange of the copies ν^i between the nodes for to guarantee that all the copies are identical. The consensus algorithm [14] is executed after each subgradient iteration using:

$$\nu_i^c[k] = \frac{1}{N}\left(\nu_i[k] + \sum_{j\in\mathcal{N}_i} \hat{\nu}_j^i[k]\right), \quad \forall i \in \mathcal{N}, \tag{22}$$

where $\hat{\nu}_j^i$ refers to the last received copy at the node i of ν^j from the node j.

In order to reduce the communication load, we next introduce the idea of event triggered communication. A simple event-triggered protocol is defined with respect to the evolution of the local state, where the event-triggered condition traces the difference between the updated and the last transmitted state. Intuitively, the data (e.g. the ν-variables) are exchanged only if they possess a sufficiently high level of the novelty as compared to the most recent information transmission. In this sense, exchanging the dual variables is controlled by the event-triggered condition which computes the difference between the most recent updated ν^i and the last transmitted $\hat{\nu}^i$. Then, the event-triggered condition reads:

$$\left\|\nu^i[k+1] - \hat{\nu}^i[k]\right\| \geq \beta_0 \left\|h^i[k]\right\| + \beta_1, \quad i \in \mathcal{N} \tag{23}$$

i.e. data (ν- and F-variables) are broadcasted from the node i if the latter condition holds true, otherwise no transmission takes place. The overall algorithm involves now an iteration of three subsequential steps: subgradient updates, event-triggered data exchange and average consensus, and is shown in the table below. Note that this algorithm will serve as the reference to the scheme introduced in the next section.

Require: Exchange F_{xi}, F_{yi}, ν^i, $\forall i \in \mathcal{N}$
  while Subgradient loop **do**
   Update $\eta_i, F_{xi}, F_{yi}, \lambda_i, \sigma_i, \nu^i$
    if $\left\|\nu^i[k+1] - \hat{\nu}_i[k]\right\| \geq \beta_0 \left\|h^i[k]\right\| + \beta_1$ **then**
     RTS$_i \leftarrow$ Active
    end if
    if Active(RTS$_i$) **then**
     Transmit ν^i, F_{xi}, F_{yi}
    end if
   Node *i* receives $\hat{\nu}^j, \hat{F}_{xj}, \hat{F}_{yj}$, $\forall j \in \mathcal{N}_i$
   Consensus $\nu_i^c = \frac{1}{N}\left(\nu_i[k] + \sum_{j\in\mathcal{N}_i} \hat{\nu}_j^i\right)$
   end if

IV. TDMA PROTOCOL BASED ON SENSITIVITY ANALYSIS

A. Sensitivity analysis

The underlying implementation of the distributed optimization requires exchange of the local copies ν^i of the global variable ν, as well as the local force components F_{xi} and F_{yi} between the nodes $i \in \mathcal{N}$. We now devise an algorithm for the design of event-triggered communication, which is based on the sensitivity analysis. Hereby, we consider the information exchange of force vectors and ν-copies between the nodes as the "perturbing parameters" of the optimization iterative difference equation inferred by the subgradient algorithm. Their effect is next analyzed by means of the sensitivity analysis, e.g. see [15].

Sensitivity analysis describes the effect of a "perturbing parameter" received from the neighbors $j \in \mathcal{N}_i$ on the solution of the sub-problem *i*. We compute the sensitivity of the local variables ν^i with respect to the received variable ν^j, F_{xj} and F_{yj}, which are received from a neighbor *j*. According to the deliberation in the previous section, these variables affect explicitly the evolution of ν^i. The force components F_{xj} and F_{yj} will affect namely the subgradient vector h^i, while ν^j has an impact via the average consensus.

Recall that the subgradient update step followed by an average consensus for the Lagrange variables associated with the equality constraints can be formally given by:

$$\nu^i[k{+}1] = \frac{1}{N}\left(\nu^i[k] - \alpha \cdot h^i(F_{xi}^*[k], F_{yi}^*[k], f^j[k]) + \nu^j[k]\right),$$

where for convenience we assume $\mathcal{N}_i = \mathcal{N}$, $\forall i$, and let f^j formally be a placeholder for the received external force variables F_{xj} and F_{yj}, and, similarly, ν^j the copy of the ν at the jth node. Given that both variables, F_{xi}^* and F_{yi}^*, depend explicitly on ν^i, as defined by (20) and (21), we may formally write the above difference equation as:

$$\nu^i[k+1] = \chi^i(\nu^i[k], \nu^j[k], f^j[k]), \tag{24}$$

where χ^i is inferred by the latter equation after substituting the symbolical expressions for the optimal solutions F_{xi}^* and F_{yi}^* from (21). Now, we are particularly interested on the effect of the received information f^j and ν^j in the evolution of ν^i. According to the sensitivity analysis we can associate to this system a system of difference equation given by:

$$S_f^i[k+1] = A^i\, S_f^i[k] + B_f^i, \tag{25}$$

$$S_\nu^i[k+1] = A^i\, S_\nu^i[k] + B_\nu^i, \tag{26}$$

where

$$S_f^i = \left.\frac{\partial \nu^i}{\partial f^j}\right|_{f^j=\hat{f}_j^i, \nu^j=\hat{\nu}_j^i} \tag{27}$$

$$S_\nu^i = \left.\frac{\partial \nu^i}{\partial \nu^j}\right|_{f^j=\hat{f}_j^i, \nu^j=\hat{\nu}_j^i} \tag{28}$$

stands for the sensitivity matrices of ν^i w.r.t. f^j and ν^j, respectively, and

$$A^i = \frac{\partial \chi^i}{\partial \nu^i}, \quad B_f^i = \frac{\partial \chi^i}{\partial f^j}, \quad \text{and} \quad B_\nu^i = \frac{\partial \chi^i}{\partial \nu^j}. \tag{29}$$

Notice that $\hat{f}_j^i$ is to be understood as the last local copy received at the ith node for the local force vectors f^j. Similarly, $\hat{\nu}_j^i$ represents the most recent copy received at the ith node for the local copy of the global variable ν at the jth node. Moreover, due to the linearity of the function χ in terms of its variables, the matrices A^i and B^i are constant. As already remarked, we consider the received dual variables ν_j at the node i in the context of the sensitivity analysis as a perturbing parameter on the computation of the local dual variables. As long as no information is received, the most recent copy $\hat{\nu}_j^i$ is utilized in the update optimization equations. In analogous manner, we introduce the notation $\hat{F}_{xj}^i$ and $\hat{F}_{yj}^i$.

The sensitivity functions S_f^i and S_ν^i provide the first-order estimates of the effect of the received variations of f^j and ν^j on the local copy of the dual variable ν^i as expressed by

$$\begin{aligned}\nu^i[k](f^j,\nu^j) = \nu^i[k](\hat{f}^j,\hat{\nu}_j^i)+ \\ +S_f^i\left(f^j[k]-\hat{f}_j^i[k]\right)+S_\nu^i\left(\nu^j[k]-\hat{\nu}_j^i[k]\right).\end{aligned} \tag{30}$$

The latter equation quantifies the effect of the reception of ν^j, as well as F_{xj} and F_{yj} into ν^i updates at the ith node. In the next step, now we want to apply these estimations for designing an event-triggered communication protocol. To compute the approximated dual variables $\tilde{\nu}_j^i[k+1]$ of the neighbors $j \in \mathcal{N}_i$ at the node i, we continuously compute the sensitivity functions S_f^i and S_ν^i w.r.t. the nodes which live in the neighborhood $\mathcal{N}_i$. However, while its computation can only take place at the ith node, it is important to clear out that the sensitivity functions are actually needed at the node j, as only there they can be used to estimate the effect of the transmission of the local variables ν^j, F_{xj}, F_{yj} (cf. (30)). Hence, in addition to transmitting ν^j, F_{xj}, F_{yj}, we, additionally, need to invoke the exchange of the sensitivity matrix functions S_f and S_ν. Clearly, this is a price that has to be payed by our sensitivity-based event-triggered communication protocol.

To finalize this section, we emphasize that the estimated impact of the variables F_{xj}, F_{yj} and ν^j at a time k on the variable ν^i at the node i as computed at the node j is done by means of the expression:

$$\begin{aligned}\tilde{\Delta}\nu_i^j[k+1] = & \\ & \hat{S}_{i,\nu}^j(\nu^j[k+1]-\hat{\nu}_j^i[k]) \\ & +\hat{S}_{i,F_x}^j(F_{xj}[k+1]-\hat{F}_{xj}^i[k]) \\ & +\hat{S}_{i,F_y}^j(F_{yj}[k+1]-\hat{F}_{yj}^i[k]).\end{aligned} \tag{31}$$

E.g., here, $\hat{S}_{i,F_x}^j$ stands for the most recent copy of the sensitivity matrix $S_{F_x}^i$ available at the node j. Similarly, are to be read other hat-designated sensitivity matrices. Then, the approximated dual variables $\tilde{\nu}_i^j[k+1]$ is computed as:

$$\tilde{\nu}_i^j[k+1] = \hat{\nu}_i^j[k] + \tilde{\Delta}\nu_i^j[k+1], \tag{32}$$

where $\hat{\nu}_i^j[k]$ is the last transmitted state of node j known by node i. Each node computes the approximated dual variables of its neighbors and performs the event-triggered condition.

B. Event-triggered condition

The event-triggered condition of the node j is based on how the transition of the dual variables ν^j will affect the convergence of the distributed optimization problem at the node i, i.e. the evolution of ν^i. In particular, the transmission of the dual variables will affect its neighbors' solutions,. Therefore, we invoke the concept of the approximated dual variable $\tilde{\nu}_i^j$, which represents an estimation of the variable ν^i, as seen from the node j. We introduce the sensitivity-based event-triggered condition now as follows:

$$\left\|\tilde{\Delta}\nu_i^j[k+1]\right\| \geq \beta_0\left\|h^j\right\| + \beta_1, \tag{33}$$

where $0 < \beta_0 \leq 1$ and $0 < \beta_1 < 0.01$ are the triggering parameter which tune the acceptability of the error level. In other words, if this condition is violated, then a transmission request for ν^j, F_{xj}, F_{yj}, as well as the corresponding sensitivity matrices $S_{\nu^i}^j$, $S_{F_x}^j$, $S_{F_y}^j$, $\forall i \in \mathcal{N}$, is initiated. Generally, it is important to keep in mind that in the due of presentation of our sensitivity-based TDMA algorithm we do consider the node j as the sender and the node i as the receiver of the information at hand. For the sake of simplicity, we hereby suggest a broadcast rather than peer-to-peer communication. Indeed, broadcasting the sensitivity matrices represents an overhead for the protocol deployment.

C. Adaptive TDMA scheduler

If the event-triggered condition (33) is fulfilled, the node sends a transmission request to the TDMA scheduler, acquiring a time slot in the next frame. The scheduler adapts the number of time slots within the TDMA frame based on the number of transmission requests, and also regulates the channel utilization time assigned within each slot. Using a fixed TDMA frame in conjunction with an event-triggered scheme will not improve channel time utilization, because the time slot will be reserved for the node even if its event-triggered condition was not fulfilled. Therefore, the assignment of time slots will be conducted according to the node transmission request which activated by the event-triggered scheme.

In the proposed adaptive TDMA scheduler, the number of time slots per frame is equal to the number of transmission requests. Considering that a TDMA-based wireless network consists of N nodes, it is obvious that each TDMA frame includes $T_s = N$ time slots. In contrast, in the adaptive TDMA scheduler, the TDMA frame consists only of N_t time slots, with N_t being the number of nodes that satisfy the event-triggered condition. Practically, the adaptive event-triggered TDMA scheduler fits a large wireless network where the number of interconnected node is more than the allowable number of time slots per frame.

D. System structure

A wireless networked system consisting of $\mathcal{N} = \{1,\ldots,N\}$ nodes are connected through a TDMA protocol [16]. Each node is equipped with a local solver of the optimization problem, and it consists of a dual subgradient

Nomenclature

primal variables	η_i, F_{xi}, F_{yi}
local dual multiplier variables	$\nu^i, \lambda_i, \sigma_i$
global dual variable assoc. with $h = 0$	ν
last transmitted dual variables	$\hat{\nu}^i, \hat{\nu}^j$
consensus dual variable	ν^c
approximation of ν^i at node j	$\tilde{\nu}_i^j$
approximated increments of $\tilde{\nu}_i^j$	$\tilde{\Delta}\nu_i^j$
event-triggered parameters	β_0, β_1
sensitivity functions	S_f^i, S_ν^i
recent copies of sensitivity matrices at node j	$\hat{S}_{i,\nu}^j, \hat{S}_{i,F_x}^j, \hat{S}_{i,F_y}^j$
transmitted variables	ν^j, F_{xj}, F_{yj}
last transmitted ν^i	$\hat{\nu}^i$
most recent received ν^i at node j	$\hat{\nu}_i^j$

algorithm and an event-triggered scheme that links the application and communication layers. The event-triggered policy regulates the nodes' transmission request, and the triggering condition is computed by utilizing the sensitivity analysis of the effect of transmission the node's dual variables on its neighbors' problem solution. The TDMA scheduler divides the channel time with respect to the number of connected nodes, and assigns each node with time slot in continuous order. More specifically, we consider a system depicted in Fig. 2, it consists of wireless network with $N = 4$ nodes forming one vehicle cluster, and it operates based on TDMA protocol. The channel time is divided into N_f frames equal to the number of solver iterations, and each frame consists of $T_s = N$ time slots with a fixed time Δ_t time unit, and each node is assigned with time slot $T_{s,i}$ in continuous order according to the available time slots per frame.

Require: Exchange $\nu^i, F_{xi}, F_{yi}, S_\nu^i, S_{F_x}^i, S_{F_y}^i, \forall i \in \mathcal{N}$
while Subgradient loop **do**
Update: $\eta_i, F_{xi}, F_{yi}, \nu^i, \lambda_i, \sigma_i$
Compute sensitivity matrices:
$S_{F_x}^i[k+1] = A^i\, S_{F_x}^i[k] + B_{F_x}^i$
$S_{F_y}^i[k+1] = A^i\, S_{F_y}^i[k] + B_{F_y}^i$
$S_\nu^i[k+1] = A^i\, S_\nu^i[k] + B_\nu^i$
Compute approximated change $\tilde{\Delta}\nu_i^j[k+1]$ at a $j \in \mathcal{N}_i$
if $\left\|\tilde{\Delta}\nu_i^j[k+1]\right\| \geq \beta_0 \left\|h^j\right\| + \beta_1$ **then**
$RTS_j \leftarrow$ Active
end if
if Active(RTS_j) **then**
Transmit ν^j, F_{xj}, F_{yj}, S_ν^j, $S_{F_x}^j$, $S_{F_y}^j$
end if
Node i receives: ν^j, F_{xj}, F_{yj},S_ν^j, $S_{F_x}^j$, $S_{F_y}^j$, $\forall j \in \mathcal{N}_i$
Consensus: $\nu_i^c = \frac{1}{N}\left(\nu_i[k] + \sum_{j \in \mathcal{N}_i} \hat{\nu}_j\right)$
end while

V. Simulation and Discussion

The performance of the proposed algorithms is compared with the centralized optimization problem result, where the computed solution of the adhesion potential η_i and the Lagrange multipliers $\nu_1, \nu_2,$ and, ν_3 are compared with the optimal solution. By "centralized optimization", we define the scenario, where a special ECU is dedicated for the accommodation of the evolution of the global ν-variables. That is, we dispense with its local copies ν^i. This algorithm has been introduced in Section III.A).

First, we show the simulation result of the distributed optimization problem, followed by the simulation result of the adaptive TDMA sensitivity based algorithm. A lane change maneuver under braking is used as a reference trajectory for the vehicle dynamics optimization problem, and the parameters of the maneuver scenario are defined with maximum longitudinal deceleration of $a_x \approx 3$ [m/s^2] and maximum lateral acceleration of $a_y \approx 8$ [m/s^2] at a speed of $v = 80[km/h]$ under dry road conditions with $\mu_{max} = 1$.

Fig. 3 compares the distributed problem solution with the optimal solution of the centralized problem, and it shows the absolute error of the distributed η_i compared with the centralized solution. The simulation shows a good performance of the distributed algorithm even in the critical driving scenario, and the absolute error is decreased dramatically in simple maneuver instance, and acceptable in difficult one. Fig. 5 presents the convergence of the local dual multipliers ν_i^c with respect to the global dual multiplier ν computed by a centralized solver algorithm. The simulation shows a complete convergence of both variables even in a critical maneuver instance.

In order to evaluate the proposed sensitivity-based event-triggered adaptive TDMA algorithm, the algorithm is implemented in four nodes communicate over wireless network base on TDMA protocol. We point out that the simulation study considers the convergence of the distributed optimization problem with respect to the adaptive TDMA communication protocol. The TDMA based wireless network is simulated as additive white Gaussian noise channel, and the SNR is randomly distributed over the frequency and time with maximum value up to 130 dB. The efficiency of the proposed algorithm is evaluated in terms of the

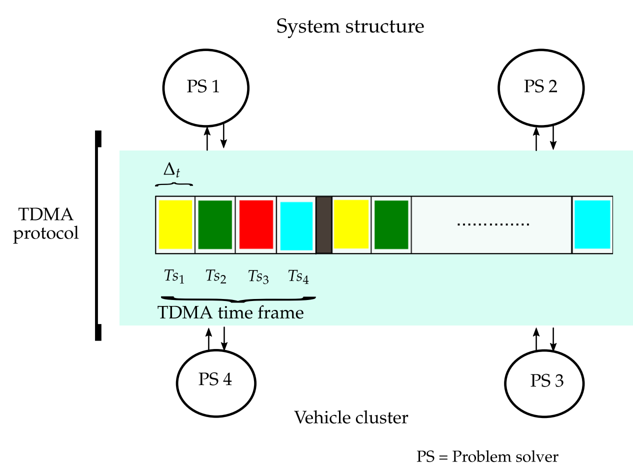

Fig. 2. Event-triggered TDMA protocol structure. To the underlying application, the PS1-4 represent, e.g. the ECUs mounted on the individual vehicle wheels that overtake steering the vehicle along a predefined maneuver.

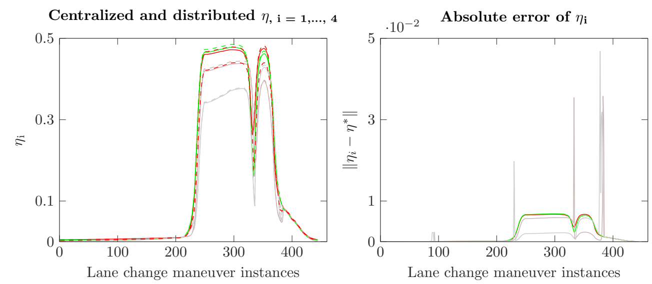

Fig. 3. The distributed algorithm performance compared with centralized (left), and the absolute error of the distributed η_i (right).

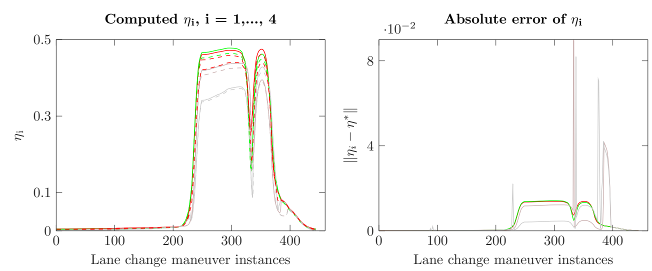

Fig. 4. Algorithm performance over the complete maneuver: computed adhesion potential η_i for all nodes (left) and absolute error (right). The relative error increases in the case of difficult maneuvers.

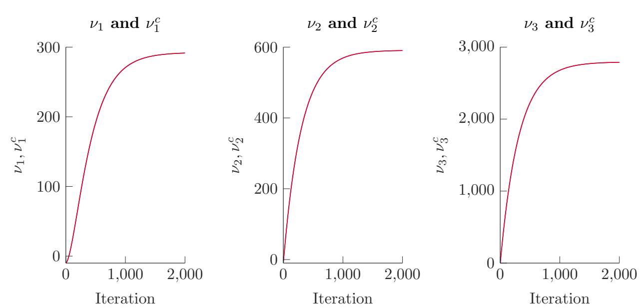

Fig. 5. The behavior of the distributed dual variables ν_i^c compared with the global variables ν of the centralized optimization for a critical maneuver instance (250th in Fig. 3).

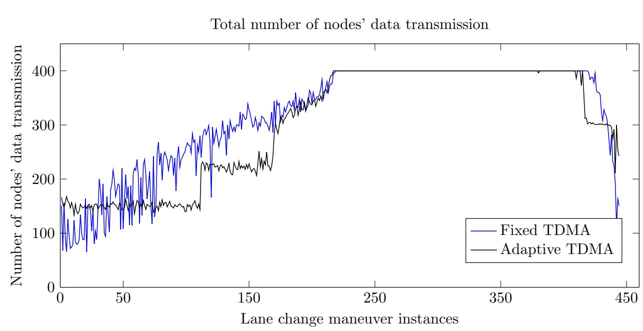

Fig. 6. The net communication activities of all nodes.

communication reduction in relation to the convergence of the distributed optimization problem, and the absolute error rate caused by the reduction of the communication caused by event-triggered scheme.

The application layer consists of one vehicle cluster consisting of $N = 4$ nodes, which internally equipped with an event-triggered subgradient solver of the optimization problem of the vehicle dynamics. The event triggered scheme

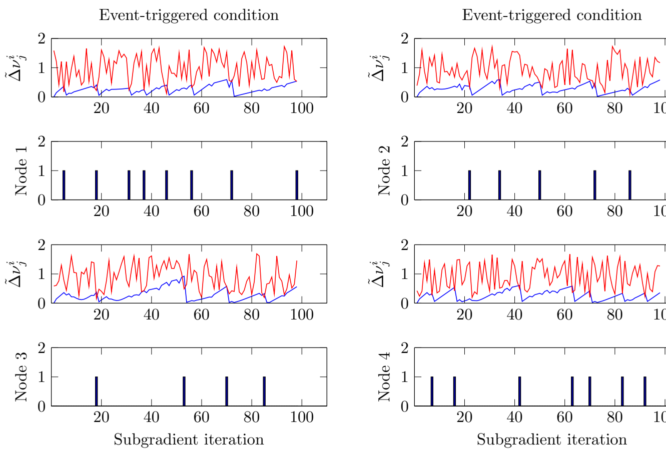

Fig. 7. Performance of the event-triggered condition $\left\|\tilde{\Delta}\nu_i^j[k+1]\right\|$ w.r.t the triggering threshold $\beta_0 \left\|h^j\right\| + \beta_1$, cf. (33), for a maneuver sample with rather low communication load.

parameters are set to $\beta_0 = 0.03$ and $\beta_1 = 0.0001$ which are chosen to guarantee the optimal performance of the distributed algorithm, and the dual subgradient method is updated with a fixed step size $\alpha = 0.04$, and runs for 150 subgradient update iteration steps.

The convergence rate of the distributed optimization problem was computed according to the relative error $= \frac{\|\eta_i - \eta^*\|}{\|\eta^*\|}$, the relative error traces the performance of the proposed algorithm by computing the convergence rate of η_i with respect to η_i^* computed by the centralized algorithm. Following the evaluation criterion from our previous work, we start with a full maneuver simulation in order to evaluate the algorithms performance with different driving scenarios including moderate and extreme maneuver. Fig. 4 presents the computed adhesion potential η_i for $\{i = 1, ..., 4\}$ nodes, and also shows the absolute error $\|\eta_i - \eta^*\|$ computed with reference to the optimal η^*. We see that the algorithms performance is highly improved, as it provides a nearly accurate η_i value with respect to optimal adhesion potential η^*, and we notice noticeable decrease in the absolute error value in the case of simple, and moderate maneuver instances. Therefore, the sensitivity-based even-triggered scheme maintains the system performance with respect to the computation of η_i also in instances of extreme driving maneuvers.

Fig. 6 compares the communication activities within the network of the adaptive TDMA and fixed TDMA protocol of the complete lane change maneuver and it shows a noticeable reduction in communication activities up to 70% in the simple and moderate maneuver instances, and we see a noticeable communication reduction in the case of the adaptive TDMA protocol. The event-triggered scheme regulates the transmission request and provides an efficient use of the communication resources.

Fig. 7 presents the performance of the event-triggered condition $\left\|\tilde{\Delta}\nu_i^j[k+1]\right\|$ with respect to the threshold $\beta_0 \left\|h^j\right\| + \beta_1$, and it shows the communication activities for each node. We see that the node broadcasts its state update if

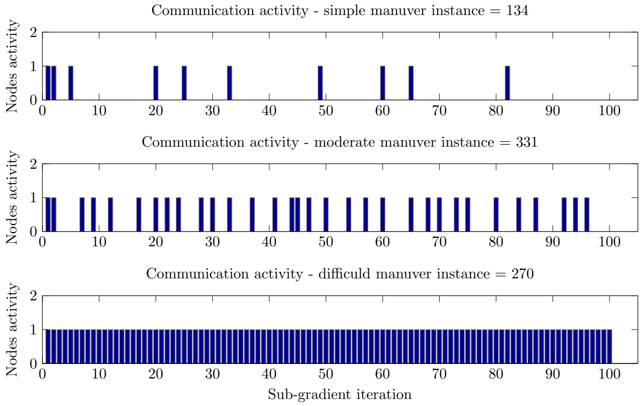

Fig. 8. Communication activities: Node communication is reduced in simple maneuver instance, quietly reduced in moderate maneuver instance, and no reduction difficult maneuver case.

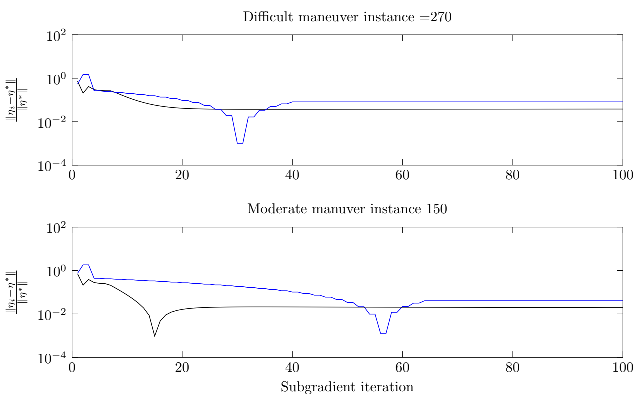

Fig. 9. Convergence rate in extreme and moderate maneuver instance for event-triggered algorithms based on the local increments (Algorithm Section III-B, blue plots) and on estimated increments about the nodes in environment (Algorithm Section IV, black plots).

the triggering condition reaches the acceptable error level regulated by the triggering threshold. On the other hand, the event-triggered threshold depends on the equality constraint $h^j = 0$, which is sensitive to the changes in other nodes' state variables. As we see, the proposed sensitivity event-triggered algorithm leads to a communication reduction between the nodes. Notice that, in the extreme maneuver instance, nodes require higher communication rate in order to converge to the optimal value. Therefore, the event-triggered condition will try to reduce the communication request. Fig. 8 shows the communication activities of all nodes in the case of simple, moderate, and difficult maneuverer instances. We observe that the communication is reduced dramatically in the simple and moderate maneuver instances. while in the extreme maneuver, the communication is not reduced because the solution algorithm requires more data exchange in order to converge to the optimal value.

Finally, Fig. 9 presents the convergence rate of the extreme and moderate maneuver instances. We see that the distributed problem converges slower in the case of extreme maneuver instance, and converges faster in the moderate case with reduced error in the computed η_i.

VI. Conclusions

In this paper, we presented a sensitivity-based event-triggered adaptive TDMA protocol with application to vehicle dynamics as a benchmark. The tracked sensitivity functions were used to approximate the effect of transmission of the state update of the node on the neighbors' states, this representing the basis of our event-triggered condition for a transmission request. The simulation results demonstrate that the proposed protocol achieves an acceptable communication reduction and it also maintains the system performance even during critical driving maneuvers, which are typically associated with high communication demands. Additionally, we consider event-triggered algorithms based on local state increments. The analysis is completed in informal manner by extensive simulation in various scenarios. Finally, we extend the algorithm for optimal tire force allocation in the setting reflecting minimization of the tire adhesion.

References

[1] P. Tabuada. Event-triggered real-time scheduling of stabilizing control tasks. *Automatic Control, IEEE Transactions on*, 52(9):1680–1685, Sept 2007.

[2] P. Wan and M. Lemmon. Distributed network utility maximization using event-triggered augmented Lagrangian methods. In *Proceedings of the 2009 conference on American Control Conference*, ACC'09, pages 3298–3303, Piscataway, NJ, USA, 2009. IEEE Press.

[3] W. Heemels, K. Johansson, and P Tabuada. An introduction to event-triggered and self-triggered control. In *CDC*, pages 3270–3285, 2012.

[4] M. Miskowicz. Send-on-delta concept: An event-based data reporting strategy. *Sensors*, 6(1):49, 2006.

[5] T. Gommans and W. Heemels. Resource-aware mpc for constrained nonlinear systems: A self-triggered control approach. *Systems and Control Letters*, 79:59–67, May 2015.

[6] F. Brunner, T. Gommans, W. Heemels, and F. Allgower. Communication scheduling in robust self-triggered MPC for linear discrete-time systems. In *IFAC Workshop on Distributed Estimation and Control in Networked Systems (NECSYS) 2015, Philadelphia, USA*, 2015.

[7] S. Guma and N. Bajcinca. Distributed feedforward control of vehicle dynamics based on event-triggered optimization. In *Information, Communication and Automation Technologies (ICAT), 2013 XXIV International Symposium on*, pages 1–6, Oct 2013.

[8] N. Bajcinca and Y. Kouhi. Distributed optimization for feedforward global chassis control. In *IFAC Symposium on Advances in Automotive Control*, Munich, 2010.

[9] R. Madan and S. Lall. Distributed algorithms for maximum lifetime routing in wireless sensor networks. In *Global Telecommunications Conference, 2004. GLOBECOM '04. IEEE*, volume 2, pages 748–753 Vol.2, Nov 2004.

[10] Y. Kouhi, S. Guma, and N. Bajcinca. Real-time allocation of tire adhesion forces for electric vehicles. In *Control Applications (CCA), 2012 IEEE International Conference on*, pages 172–177, 2012.

[11] M. Villella. Nonlinear modeling and control of automobiles with dynamic wheel-road friction and wheel torque inputs. In *IFAC Symposium on Advances in Automotive Control*, 2004.

[12] R. Orend. Steuerung der ebenen Fahrzeugbewegung mit optimaler Nutzung der Kraftschlusspotentiale aller vier Reifen. *Automatisierungstechnik*, 53(1):20–27, 2005.

[13] X. Wang and M. Lemmon. Event-triggering in distributed networked control systems. *IEEE Trans. Automat. Contr.*, 56(3):586–601, 2011.

[14] K. Avrachenkov, M. ElChamie, and G. Neglia. A local average consensus algorithm for wireless sensor networks. In *Distributed Computing in Sensor Systems and Workshops (DCOSS), 2011 International Conference on*, pages 1–6, June 2011.

[15] H. Khalil. *Nonlinear systems*. Prentice Hall, Upper Saddle River (New Jersey), 2002.

[16] T. Herman and S. Tixeuil. *A distributed TDMA dlot assignment algorithm for wireless sensor networks*. Springer Berlin Heidelberg, Berlin, Heidelberg, 2004.